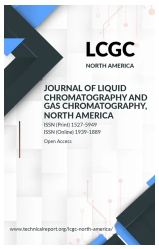

Journal of Liquid Chromatography and Gas Chromatography, North America
https://technicalreport.org/lcgcnam

LC GC N. Am., Vol. 44, No.1, 08-13, 2026

Technical Reports Press

RESEARCH ARTICLE

Retention–Fragmentation Biosynthetic Fingerprinting of Engineered Kdo_2-Monophosphoryl Lipid A Variants

Michael P. Doyle[1*] **and Sayan Pratab**[1]

[1] *Department of Chemistry, The University of Texas at San Antonio, San Antonio, TX 78249, United States*
[*] *Corresponding author*

Corresponding author:
michael.doyle@utsa.edu

Received: 20 November 2025
Accepted: 11 February 2026
Available online: 30 March 2026

Abstract

Kdo_2-lipid A and Kdo_2-monophosphoryl lipid A (Kdo_2-MPLA) connect Gram-negative outer-membrane biochemistry with the analytical design of lipopolysaccharide-derived vaccine-adjuvant candidates. Their characterization is demanding because acyl-chain number, acyl-chain position, phosphate state, Kdo substitution, and ion adduction jointly shape reversed-phase retention and tandem mass-spectrometric fragmentation. This study establishes a retention–fragmentation biosynthetic fingerprint for eight structurally assigned Kdo_2-lipid A derivatives from engineered *Escherichia coli* analyzed by triethylamine-assisted reversed-phase LC–MS/MS. Each species was encoded by acylation class, phosphate number, total acyl carbon count, secondary-acyl-chain identity, primary-chain length, precursor-adduct state, and diagnostic MS/MS evidence. A constrained two-parameter retention rule based on total acyl carbon number and phosphate count explained the observed retention ladder with high internal consistency ($R^2 = 0.992$; root-mean-square error = 0.158 min; leave-one-out mean absolute error = 0.19 min). Matched structural contrasts showed that diphosphorylation advanced elution by 0.15–0.16 min within tetra- and hexa-acylated scaffolds, whereas replacement of C13:0(3-OH) by C14:0(3-OH) delayed elution by 0.24 min in the penta-L series. Diagnostic MS/MS evidence from Kdo/Kdo_2 ions, $^{0,4}A_2$ cross-ring fragments, phosphate loss, acyl-chain loss, and adduct-dependent suppression of glycosidic cleavage separated MPLA-like, diphosphoryl lipid A (DPLA)-like, and adduct-dominated spectra. The fingerprint distinguishes target MPLA products, residual diphosphorylated species, and primary-chain microheterogeneity, giving a chemically constrained quality-control readout for Kdo_2-MPLA engineering.

Keywords: Kdo_2-lipid A; monophosphoryl lipid A; LC–MS/MS; triethylamine; lipidomics; biosynthetic fingerprinting; adduct-aware annotation; vaccine adjuvant

1. Introduction

Lipopolysaccharide (LPS) is a defining constituent of the Gram-negative outer membrane and is essential to membrane-barrier function, host–pathogen recognition, and inflammatory signaling [1–3]. Lipid A, the hydrophobic anchor of LPS, is the principal immunologically active region. Its acyl-chain number, acyl-chain length, acyl-chain position, and phosphorylation state strongly influence recognition by the TLR4–MD-2 complex and determine whether a molecule behaves as a potent endotoxin or as a detoxified immunostimulatory scaffold [4–6]. These structure–activity relationships explain the sustained interest in monophosphoryl lipid A (MPLA), Kdo-containing lipid A analogues, and biosynthetically engineered lipid A products as vaccine-adjuvant candidates [5, 7, 8].

Kdo_2-lipid A is a valuable biochemical and analytical model because it retains the inner-core 3-deoxy-D-manno-oct-2-ulosonic acid (Kdo) disaccharide attached to lipid A while avoiding much of the compositional complexity of full-length LPS [9]. It is also biosynthetically informative: late acyltransferase activity depends on Kdo substitution, and engineered changes in acyltransferases, phosphatases, or core-biosynthesis genes can shift the product distribution toward Kdo_2-MPLA analogues [10–12]. The same chemical features make the analytes technically demanding. Kdo_2-lipid A species are amphiphilic, highly anionic, structurally heterogeneous, and prone to adduct formation and pathway-dependent fragmentation in electrospray ionization mass spectrometry [13, 14].

Cite as: M.P. Doyle & S. Pratab (2026). Retention–Fragmentation Biosynthetic Fingerprinting of Engineered Kdo_2-Monophosphoryl Lipid A Variants. LC GC N. Am., 44(1) (2026) 08-13.

Triethylamine (TEA)-assisted reversed-phase LC–MS/MS improves the separation and structural assignment of Kdo_2-lipid A derivatives by combining volatile ion pairing, high-resolution negative-ion detection, and stepped-collision-energy parallel-reaction-monitoring spectra [14]. The assigned LC–MS/MS record contains eight Kdo_2-lipid A species from engineered *E. coli*, spanning tetra-, penta-, and hexa-acylated MPLA and DPLA structures. It also contains diagnostically important Kdo and Kdo_2 product ions, $^{0,4}A_2$ cross-ring fragments, phosphate losses, acyl-chain losses, and adduct-specific fragmentation behavior.

A central analytical challenge is to interpret the product pattern rather than only identify isolated peaks. Engineered lipid A systems commonly generate product distributions. Residual diphosphorylated species, altered primary-chain lengths, and adduct-dependent spectra may indicate incomplete conversion, enzyme-substrate flexibility, or quality-control risks in adjuvant-oriented lipid A engineering. A coherent retention–fragmentation readout is therefore needed to connect chromatographic order, MS/MS evidence, and biosynthetic interpretation.

The contribution of this study is the conversion of eight assigned Kdo_2-lipid A species into a chemically interpretable pathway-level fingerprint. The study (i) recodes each assigned species into explicit structural descriptors, (ii) tests a minimal retention rule against internal chromatographic contrasts, (iii) organizes diagnostic MS/MS evidence into an adduct-aware classification sequence for MPLA-like, DPLA-like, and adduct-dominated spectra, and (iv) maps the assigned products into target MPLA, residual diphosphorylated, and primary-chain-variant classes. This integrated readout supports quality-control interpretation of Kdo_2-MPLA engineering without overextending the available LC–MS/MS evidence.

2. Materials and methods

2.1. Experimental record and inclusion criteria

The experimental basis comprised the LC–MS/MS assignments of Kdo_2-lipid A and Kdo_2-MPLA derivatives isolated from engineered *E. coli* strains as described by [14]. The separation used a YMC-Triart C18 column with TEA-containing mobile phases under basic reversed-phase conditions. Mobile phase A consisted of methanol/water containing TEA and acetic acid, and mobile phase B consisted of isopropyl alcohol containing TEA and acetic acid. Negative-ion heated electrospray ionization was used; full-scan spectra were acquired at high resolution; and targeted MS/MS spectra were collected by parallel reaction monitoring with a narrow isolation window and stepped collision energies of 20, 40, and 60 eV [14].

The analytes included here were the eight Kdo_2-lipid A species for which retention time, calculated and measured doubly deprotonated mass, mass deviation, acyl-chain assignment at C3′, C2′, C3, and C2, and biosynthetic expectation were available. Diagnostic MS/MS evidence was coded from the assigned fragment interpretation, including Kdo and Kdo_2 ions, $^{0,4}A_2$ ring-cleavage ions, phosphate-loss behavior, acyl-chain losses, and precursor-adduct spectra. Because replicate chromatographic peak areas and biological-response measurements were not part of the assigned record, validation was restricted to internal chemical consistency across orthogonal observables.

2.2. Structural encoding

Each species was encoded using descriptors that are chemically interpretable and directly recoverable from the structural assignments: acylation number, phosphate number, total acyl carbon count, number of C12 secondary acyl chains, number of C14 secondary acyl chains, presence of a shortened C13 primary hydroxyacyl chain, and biosynthetic class. The total acyl carbon count was defined as

$$C_{\mathrm{acyl},i} = \sum_{j=1}^{n_i} c_{ij}, \tag{1}$$

where n_i is the number of acyl chains in species i and c_{ij} is the carbon number of acyl chain j. Hydroxylation was not included as a separate term because the available contrasts are driven primarily by acyl number, chain length, secondary acylation, and phosphate number, whereas hydroxy substitution is largely shared across the primary chains.

2.3. Retention model and internal validation

Retention was modeled with a constrained structure–retention rule. Because only eight assigned species were available, a high-dimensional regression would be unstable and would weaken chemical interpretation. The selected rule used total acyl carbon count and phosphate number:

$$\mathrm{RT}_i = \beta_0 + \beta_1 C_{\mathrm{acyl},i} + \beta_2 P_i + \varepsilon_i, \tag{2}$$

where RT_i is retention time in minutes and P_i is the number of phosphate groups. The expected chemical direction is positive for C_{acyl}, because additional acyl carbon increases reversed-phase retention, and negative for P, because additional phosphate increases polarity and reduces apparent hydrophobicity under TEA-assisted conditions.

Ordinary least-squares coefficients were calculated from the encoded table. Internal validation used four complementary checks: coefficient direction, residual structure, leave-one-out prediction error, and pairwise isostructural contrasts. The pairwise checks compared tetra-DPLA with tetra-MPLA, hexa-M-L-DPLA with hexa-M-L-MPLA, and penta-L-MPLA′ with penta-L-MPLA. These checks determine whether the retention rule is chemically coherent within the assigned set; they do not imply population-level predictive performance for unmeasured lipid A analogues.

2.4. MS/MS evidence coding

MS/MS annotations were coded into a diagnostic classification sequence. Six evidence classes were used: (i) Kdo/Kdo_2 product ions around m/z 219 and 439; (ii) $^{0,4}A_2$ ring-cleavage ions around m/z 508 and 690; (iii) doubly charged losses of Kdo residues or Kdo_2; (iv) acyl-chain losses as acid or ketene fragments; (v) phosphate loss; and (vi) precursor-adduct identity. A confident assignment requires agreement among precursor mass, retention position, phosphorylation evidence, acyl-loss evidence, and adduct-specific fragmentation behavior.

2.5. Pathway classification

Species were classified into three pathway-relevant groups: target MPLA products, residual diphosphorylated products, and primary-chain variants. A target MPLA product was defined by an acylation and phosphorylation pattern consistent with engineered late-acyltransferase and lipid A phosphatase activity. A residual diphosphorylated product was defined by retention of two phosphate groups in a product series designed to enrich MPLA species. A primary-chain variant was defined by a chain-length difference within an otherwise matched acylation pattern. These classes are analytical and mechanistic; confirmation of enzymatic flux would require replicate abundance measurements, enzyme-expression data, and targeted biosynthetic experiments.

3. Results

3.1. The LC–MS/MS assignments contain separable structural and biosynthetic signals

The eight assigned Kdo_2-lipid A species span three acylation classes, two phosphorylation states, and multiple secondary-acyl-chain patterns. Table 1 reorganizes the assignments into the structural variables used for retention, fragmentation, and pathway interpretation. The species include tetra-acylated DPLA and MPLA, three penta-acylated MPLA variants, two hexa-acylated MPLA variants, and one hexa-acylated DPLA species.

The encoded assignments contain informative internal contrasts. Species A and B have the same acyl carbon count but differ in phosphate number. Species G and H share a high-carbon hexa-acylated scaffold but differ in phosphate number. Species C and D differ mainly by a one-carbon shortening of the primary chain at C3′. These contrasts allow retention and fragmentation behavior to be evaluated as chemically linked features rather than as isolated peak annotations. Figure 1 summarizes how descriptor encoding, retention behavior, product-ion evidence, and pathway class were integrated.

3.2. Retention follows a constrained hydrophobicity–phosphate rule

The retention order is consistent with increasing hydrophobicity. Within MPLA species, tetra-acylated Kdo_2-MPLA eluted at 3.21 min, penta-acylated species eluted at 5.30–6.11 min, and hexa-acylated species eluted at 7.30–7.73 min. Additional acyl chains therefore increased interaction with the reversed-phase stationary phase. Phosphate number modulated this trend: Kdo_2-tetra-DPLA eluted before the matched tetra-MPLA species despite having the same acyl carbon count, and Kdo_2-hexa-M-L-DPLA eluted before Kdo_2-hexa-M-L-MPLA despite sharing the same total acyl carbon count.

The fitted retention rule was

$$\widehat{\mathrm{RT}} = -5.885 + 0.1708 C_{\mathrm{acyl}} - 0.2937 P. \quad (3)$$

Within the eight-species set, the rule gave $R^2 = 0.992$, root-mean-square error of 0.158 min, and leave-one-out mean absolute error of 0.19 min (Figure 2). The coefficient signs match the expected chemistry: each additional acyl carbon increases retention, whereas each additional phosphate reduces retention under the TEA-assisted reversed-phase conditions. The fitted phosphate coefficient represents the global least-squares effect after adjustment for acyl carbon count; the directly matched phosphate contrasts were smaller and highly consistent.

The pairwise contrasts support the fitted rule. In the tetra-acylated pair, the additional phosphate in Kdo_2-tetra-DPLA advanced elution by 0.15 min relative to Kdo_2-tetra-MPLA. In the hexa-acylated M-L pair, the additional phosphate advanced elution by 0.16 min. The agreement between low-carbon and high-carbon scaffolds supports a consistent phosphate-state effect within the method. In the penta-L pair, replacement of C13:0(3-OH) by C14:0(3-OH) at C3′ delayed elution by 0.24 min, consistent with a one-carbon increase in hydrophobicity. The larger 0.57 min shift from penta-L-MPLA to penta-M-MPLA reflects both a two-carbon increase and altered secondary-acyl-chain identity.

3.3. Retention residuals reveal topology-dependent effects

Although the two-variable rule captures the dominant retention trend, the residuals identify structural features not fully represented by carbon count and phosphate number. Kdo_2-penta-M-MPLA produced the largest positive residual, eluting approximately 0.33 min later than predicted. This suggests that secondary C14:0 acylation at C3′ increases reversed-phase retention more strongly than a simple carbon-count term captures. Kdo_2-hexa-L-MPLA and Kdo_2-tetra-MPLA eluted earlier than predicted by approximately 0.19 and 0.18 min, respectively, indicating that acyl topology, ion-pair geometry, and phosphate exposure contribute additional selectivity.

These residuals are chemically informative. The carbon-count term describes the major hydrophobic trend, whereas residual structure points to the influence of secondary-acyl-chain position, phosphate accessibility, and molecular conformation. In a larger assigned set, these deviations could support a refined quantitative structure–retention relationship. In the present set, they identify where lipid A topology modifies bulk hydrophobicity and where retention information should be interpreted with fragment-level evidence.

3.4. Diagnostic fragments support adduct-aware classification

The stepped-collision-energy MS/MS spectra contain diagnostic evidence that can be ordered into a structured annotation sequence (Figure 3). The first layer confirms Kdo_2-lipid A identity through Kdo and Kdo_2 product ions around m/z 219 and 439. The second layer separates MPLA-like and DPLA-like behavior. In MPLA spectra, $^{0,4}A_2$ cross-ring fragments around m/z 508 and 690 support the absence of a C1 phosphate and provide information about C2′ acyl substitution. In DPLA spectra, the absence of this ring-cleavage pattern, together with serial Kdo losses, phosphate loss, and ketene loss from the C3′ acyl chain, supports diphosphorylated assignment. The third layer evaluates acyl-chain topology using acid or ketene losses associated with C3 and C3′ positions.

This sequence addresses a common ambiguity in lipid A MS/MS interpretation. Individual fragments may not be position-specific, and adducts can suppress glycosidic cleavage that would otherwise be diagnostic. Reliable annotation therefore requires agreement among multiple evidence classes. Deprotonated ions provide the richest topology information, whereas sodium, potassium, disodium, and phosphate adducts can shift the fragmentation pathway. These adducts are analytically useful when interpreted with precursor-specific expectations because they can confirm molecular weight and reveal which cleavages are stabilized or suppressed by cation or phosphate association.

3.5. Adduct behavior strengthens structural confidence

The hexa-acylated Kdo_2-M-L-MPLA species was assigned with several doubly charged precursor forms: $[M–2H]^{2-}$, $[M–3H+Na]^{2-}$, $[M–4H+2Na]^{2-}$, $[M–3H+K]^{2-}$, and $[M–H+H_2PO_4^-]^{2-}$ [14]. Their MS/MS spectra differed substantially. The disodium adduct fragmented inefficiently, whereas potassium and dihydrogen phosphate adducts produced related patterns with abundant acyl-chain-loss ions. Kdo_2 sugar fragments were weak or absent in several adduct spectra.

This behavior has two practical implications. First, weak Kdo ions do not necessarily exclude Kdo_2-lipid A identity when precursor mass, retention position, and acyl-loss evidence remain coherent for a stable adduct. Second, multiple precursor forms supporting the same molecular formula and related acyl-loss pathways provide an additional confidence layer. For engineered lipid A quality control, adduct-aware annotation reduces false rejection of valid low-abundance species and prevents overinterpretation of adduct spectra that lack adequate topology information.

3.6. The biosynthetic fingerprint separates target products, residual DPLA, and chain-length variants

Figure 4 maps the eight species by retention time, acylation number, and pathway class. Target MPLA products comprise B, D, E, F, and H, forming a coherent chromatographic series from tetra- to hexa-acylated

Table 1: Encoded Kdo_2-lipid A species used for retention–fragmentation analysis. Retention time, mass assignment, and acyl positions are from the LC–MS/MS assignments; total acyl carbon count and pathway class were derived from those assignments.

ID	Species	RT (min)	Class	P	C_{acyl}	C3′	C2′	C3	C2	Deviation (ppm)	Biosynthetic interpretation
A	Kdo_2-tetra-DPLA	3.06	tetra-DPLA	2	56	C14:0(3-OH)	C14:0(3-OH)	C14:0(3-OH)	C14:0(3-OH)	-0.87	residual diphosphorylated tetra-acyl species
B	Kdo_2-tetra-MPLA	3.21	tetra-MPLA	1	56	C14:0(3-OH)	C14:0(3-OH)	C14:0(3-OH)	C14:0(3-OH)	0.34	tetra-acyl MPLA product
C	Kdo_2-penta-L-MPLA′	5.30	penta-MPLA	1	67	C13:0(3-OH)	C14:0[3-O-(C12:0)]	C14:0(3-OH)	C14:0(3-OH)	1.14	shortened-primary-chain penta-MPLA variant
D	Kdo_2-penta-L-MPLA	5.54	penta-MPLA	1	68	C14:0(3-OH)	C14:0[3-O-(C12:0)]	C14:0(3-OH)	C14:0(3-OH)	1.13	penta-L-MPLA product
E	Kdo_2-penta-M-MPLA	6.11	penta-MPLA	1	70	C14:0[3-O-(C14:0)]	C14:0(3-OH)	C14:0(3-OH)	C14:0(3-OH)	0.41	penta-M-MPLA product
F	Kdo_2-hexa-L-MPLA	7.30	hexa-MPLA	1	80	C14:0[3-O-(C12:0)]	C14:0[3-O-(C12:0)]	C14:0(3-OH)	C14:0(3-OH)	-6.86	hexa-L-MPLA product
G	Kdo_2-hexa-M-L-DPLA	7.57	hexa-DPLA	2	82	C14:0[3-O-(C14:0)]	C14:0[3-O-(C12:0)]	C14:0(3-OH)	C14:0(3-OH)	2.15	residual diphosphorylated hexa-acyl species
H	Kdo_2-hexa-M-L-MPLA	7.73	hexa-MPLA	1	82	C14:0[3-O-(C14:0)]	C14:0[3-O-(C12:0)]	C14:0(3-OH)	C14:0(3-OH)	-7.24	hexa-M-L-MPLA product

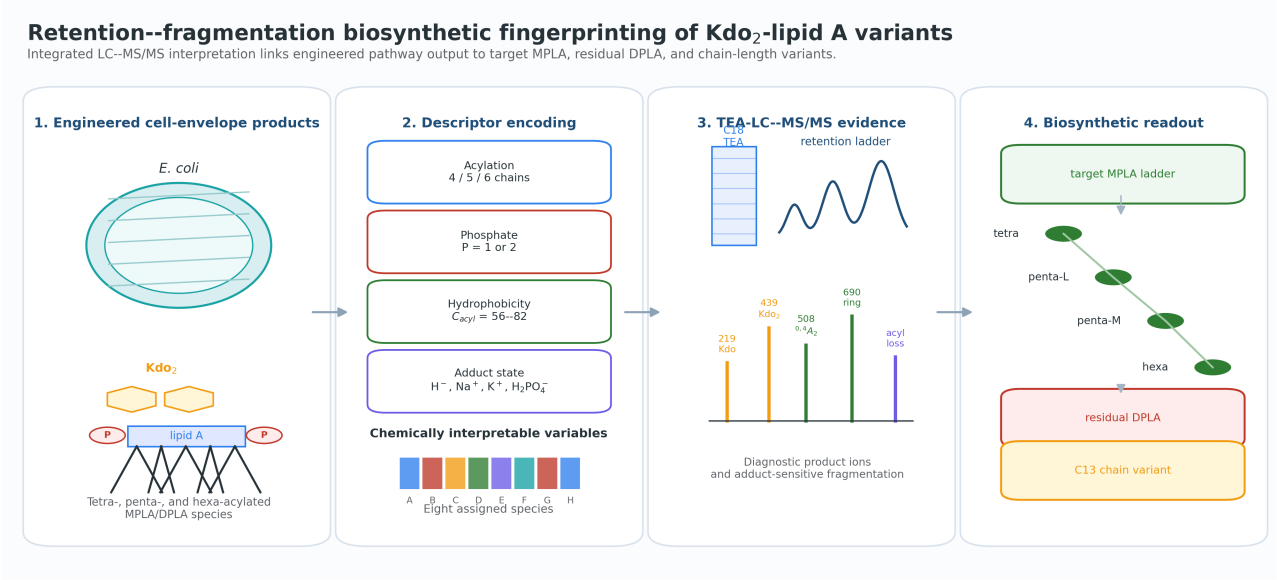

Figure 1: Integrated analytical logic for Kdo_2-lipid A biosynthetic fingerprinting. Engineered cell-envelope products are encoded by acylation, phosphate state, total acyl carbon count, and adduct form; these descriptors are interpreted jointly with retention order and diagnostic MS/MS fragments to classify target MPLA products, residual DPLA species, and primary-chain variants.

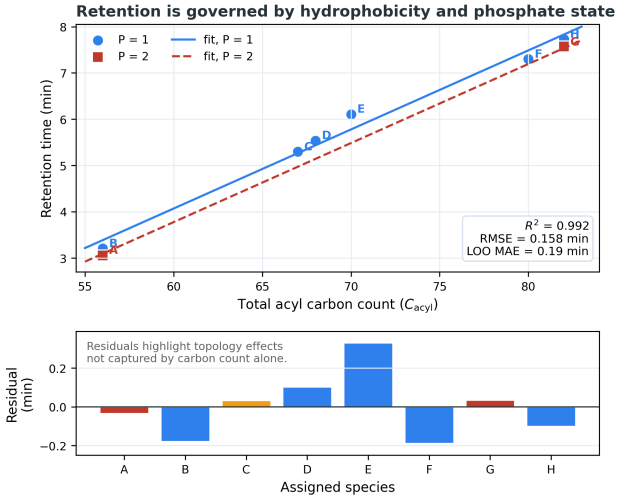

Figure 2: Retention validation for the encoded Kdo_2-lipid A species. The upper panel shows measured retention time against total acyl carbon count with fitted lines for monophosphorylated and diphosphorylated species. The lower panel shows residuals by species, indicating topology-dependent retention effects that are not fully captured by carbon count and phosphate number alone.

structures. Residual DPLA species comprise A and G; their earlier elution relative to matched or near-matched MPLA structures provides chromatographic evidence of retained diphosphorylation. The primary-chain variant C differs from penta-L-MPLA by a C13:0(3-OH) chain at C3′ and elutes slightly earlier.

The residual and variant species occupy chemically sensible positions in retention and fragmentation space. Species A is the diphosphorylated analogue of the tetra-acylated scaffold. Species G is the diphosphorylated analogue of the hexa-acylated M-L scaffold. Species C is the shortened-chain analogue of D. This pattern indicates a structured product distribution shaped by phosphatase conversion, late acyltransferase activity, and acyl-chain availability. The distinction is directly relevant to lipid A engineering because residual DPLA content and minor-chain variants can affect biological interpretation, comparability between preparations, and manufacturing quality control.

4. Discussion

4.1. Chemical meaning of the retention–fragmentation fingerprint

The main contribution is the transformation of compound-level LC–MS/MS assignments into a pathway-level retention–fragmentation fingerprint. The TEA-assisted LC–MS/MS method separated and assigned Kdo_2-lipid A species with detailed fragmentation evidence [14]. The present interpretation shows that these assignments also contain a coherent pattern of engineered pathway output. Retention encodes acylation number and phosphate state; residuals encode topology-dependent selectivity; diagnostic fragments encode Kdo identity, phosphorylation state, and acyl-chain topology; and adduct behavior defines how confidently each precursor form can be interpreted.

This contribution is important because lipid A engineering requires more than molecular-weight confirmation. A preparation may contain species with related nominal masses but different phosphate states,

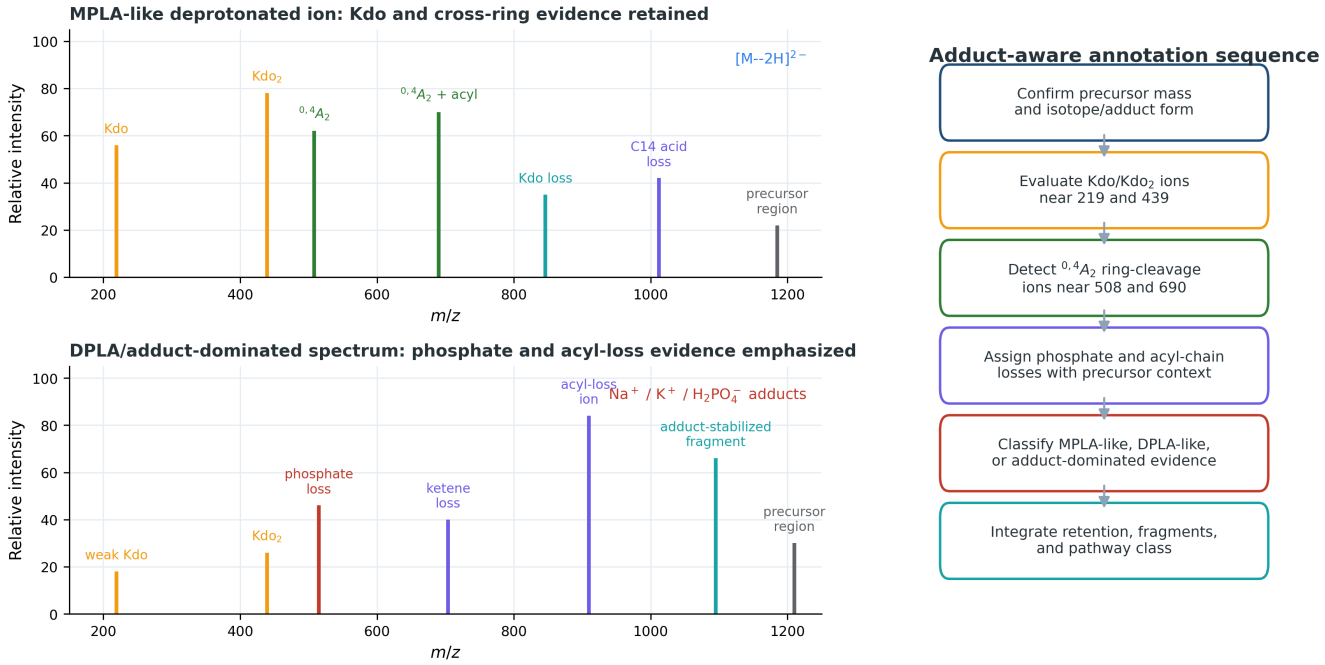

Figure 3: Adduct-aware MS/MS evidence sequence for Kdo_2-lipid A annotation. The figure compares MPLA-like deprotonated-ion spectra, DPLA/adduct-dominated spectra, and the ordered evidence classes used to integrate precursor mass, Kdo/Kdo_2 ions, $^{0,4}A_2$ fragments, phosphate loss, acyl-chain losses, and adduct-specific fragmentation.

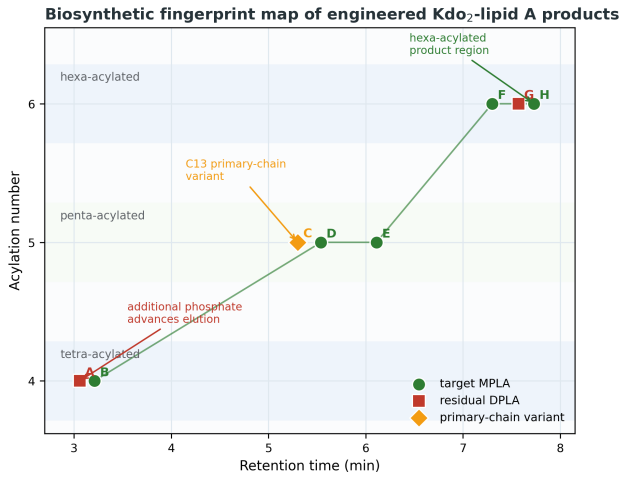

Figure 4: Biosynthetic fingerprint map of the eight Kdo_2-lipid A species. Target MPLA products define the engineered product ladder, while residual DPLA species and the C13 primary-chain variant occupy positions consistent with retained diphosphorylation or chain-length microheterogeneity.

secondary-acyl-chain positions, and adduct behavior. A retention–fragmentation fingerprint provides a compact analytical readout that links each detected species to a chemically plausible biosynthetic class.

4.2. Implications for Kdo_2-MPLA quality control

Kdo_2-MPLA engineering aims to reduce endotoxicity while retaining useful immunostimulatory activity. Because biological activity is sensitive to acyl-chain number, acyl-chain position, and phosphate state, quality control should not rely only on precursor mass or total lipid yield. The classification sequence supports a tiered strategy: confirm Kdo_2 identity, classify phosphorylation state, localize acyl topology where the spectrum permits, evaluate adduct-specific evidence, and assign the species to a target, residual, or variant product class.

This strategy is especially useful for minor species. Low-abundance products may have limited MS/MS coverage, but their retention position relative to a defined ladder provides an additional constraint. Conversely, plausible retention alone is insufficient without diagnostic fragments. The analytical strength lies in combining retention, mass accuracy, isotope/adduct coherence, and fragmentation evidence rather than relying on any single feature.

4.3. Biochemical interpretation of residual and variant products

The residual and variant products suggest three non-exclusive biochemical mechanisms. First, residual DPLA species may reflect incomplete lipid A dephosphorylation or a subpopulation of molecules less accessible to the expressed phosphatase. Second, shortened-chain penta-L-MPLA′ may reflect acyl-chain pool variation or relaxed substrate specificity during late acylation. Third, the coexistence of penta- and hexa-acylated structures indicates that acyltransferase expression and substrate availability generate a product distribution rather than a single endpoint.

These mechanisms are testable. Replicate peak-area measurements across engineered strains would determine whether the residual DPLA and short-chain species recur consistently. Time-course sampling would distinguish incomplete conversion from stable product heterogeneity. Targeted enzyme-expression measurements would evaluate whether residual diphosphorylation tracks phosphatase activity. Isotope tracing of acyl-chain uptake would test whether the C13 primary-chain variant originates from acyl-pool availability or enzyme promiscuity.

4.4. Adduct-aware annotation as an analytical requirement

Adduct formation is frequently treated as a complication in lipid MS/MS because it divides signal intensity and changes fragmentation behavior. For Kdo_2-lipid A, adduct behavior is also structurally informative. Deprotonated ions, sodium adducts, potassium adducts, disodium adducts, and dihydrogen phosphate adducts do not frag-

ment equivalently [14]. Stable adducts may suppress Kdo-glycosidic cleavage, whereas other adducts emphasize acyl-loss pathways.
An adduct-aware annotation sequence is therefore required for robust interpretation. A spectrum with weak Kdo fragments should not be rejected when the precursor is a stable adduct and the molecular weight, retention position, and acyl-loss evidence remain coherent. Conversely, adduct spectra should not be overused for complete topology assignment when they lack sufficient fragment coverage. The strongest evidence comes from integrating deprotonated-ion spectra with adduct spectra as complementary, precursor-specific views of the same molecule.

4.5. Analytical scope and validation needs

The analysis is bounded by the available assignments. The retention rule is based on eight species, so it should be used as a chemically interpretable rule for this class of analytes rather than as a universal prediction equation. Raw vendor files, replicate peak areas, and quantitative abundance measures were unavailable; therefore, product yields, conversion efficiencies, and statistical variability in product formation cannot be estimated from the present material. Biological activity was not assessed, so no conclusion is drawn about TLR4 activation, cytokine response, toxicity, or adjuvant potency.
The next validation step should acquire replicate LC–MS/MS data across engineered strains, include authentic or semisynthetic standards where available, evaluate retention transferability across columns and TEA concentrations, and link relative abundance to biological activity. The current fingerprint specifies which species, retention contrasts, fragments, and adduct states should be monitored in those experiments.

5. Conclusion

The TEA-assisted LC–MS/MS assignments of engineered *E. coli* Kdo_2-lipid A derivatives can be converted into an interpretable retention–fragmentation biosynthetic fingerprint. The eight species form a retention ladder governed mainly by total acyl carbon count and phosphate number, with residual deviations attributable to acyl topology and primary-chain length. Diagnostic MS/MS evidence, including Kdo/Kdo_2 ions, $^{0,4}A_2$ ring cleavage, phosphate loss, acyl-chain loss, and adduct-specific fragmentation, supports structured classification of MPLA-like, DPLA-like, and adduct-dominated spectra. Residual diphosphorylated species and shortened-chain variants occupy chemically meaningful positions rather than random analytical outliers. The fingerprint provides a rigorous analytical route for pathway-level quality control in Kdo_2-MPLA engineering and LPS-derived adjuvant development.

References

[1] Nikaido, H. (2003). Molecular basis of bacterial outer membrane permeability revisited. *Microbiology and Molecular Biology Reviews*, *67*, 593–656.

[2] Raetz, C. R. H., & Whitfield, C. (2002). Lipopolysaccharide endotoxins. *Annual Review of Biochemistry*, *71*, 635–700.

[3] Whitfield, C., & Trent, M. S. (2014). Biosynthesis and export of bacterial lipopolysaccharides. *Annual Review of Biochemistry*, *83*, 99–128.

[4] Park, B. S., Song, D. H., Kim, H. M., Choi, B. S., Lee, H., & Lee, J. O. (2009). The structural basis of lipopolysaccharide recognition by the TLR4–MD-2 complex. *Nature*, *458*, 1191–1195.

[5] Casella, C. R., & Mitchell, T. C. (2008). Putting endotoxin to work for us: Monophosphoryl lipid A as a safe and effective vaccine adjuvant. *Cellular and Molecular Life Sciences*, *65*, 3231–3240.

[6] Wang, B., Han, Y., Li, Y., Li, Y., & Wang, X. (2015). Immunostimulatory activity of *Escherichia coli* mutants producing Kdo_2-monophosphoryl-lipid A or Kdo_2-pentaacyl-monophosphoryl-lipid A. *PLOS ONE*, *10*, e0144714.

[7] Coler, R. N., Bertholet, S., Moutaftsi, M., Guderian, J. A., Windish, H. P., Baldwin, S. L., Laughlin, E. M., Duthie, M. S., Fox, C. B., Carter, D., Friede, M., Vedvick, T. S., & Reed, S. G. (2011). Development and characterization of synthetic glucopyranosyl lipid adjuvant system as a vaccine adjuvant. *PLOS ONE*, *6*, e16333.

[8] Wang, J., Wang, Z., Li, Y., & Wang, X. (2014). Construction and characterization of an *Escherichia coli* mutant producing Kdo_2-lipid A. *Marine Drugs*, *12*, 1495–1511.

[9] Caroff, M., & Novikov, A. (2020). Lipopolysaccharides: Structure, function and bacterial identification. *OCL*, *27*, 31.

[10] Raetz, C. R. H., Garrett, T. A., Reynolds, C. M., Shaw, W. A., Moore, J. D., Smith, D. C., Ribeiro, A. A., Murphy, R. C., Ulevitch, R. J., Fearns, C., Reichart, D., Glass, C. K., Benner, C., Subramaniam, S., Harkewicz, R., Bowers-Gentry, R. C., Buczynski, M. W., Cooper, J. A., Deems, R. A., & Dennis, E. A. (2006). Kdo_2-lipid A of *Escherichia coli*, a defined endotoxin that activates macrophages via TLR-4. *Journal of Lipid Research*, *47*, 1097–1111.

[11] Schilling, B., Hunt, J., Gibson, B. W., & Apicella, M. A. (2014). Site-specific acylation changes in the lipid A of *Escherichia coli lpxL* mutants grown at high temperatures. *Innate Immunity*, *20*, 269–282.

[12] Valvano, M. A. (2022). Remodelling of the Gram-negative bacterial Kdo_2-lipid A and its functional implications. *Microbiology*, *168*, 001159.

[13] Aissa, I., D'ornyei, A., S'andor, V., & Kil'ar, A. (2023). Complete structural elucidation of monophosphorylated lipid A by CID fragmentation of protonated molecule and singly charged sodiated adducts. *Journal of the American Society for Mass Spectrometry*, *34*, 92–100.

[14] Hong, J., Yoon, J., Jin, H., Oh, H., Chung, H. S., & Kim, K. H. (2026). Development of an ion-pairing reagent-assisted LC–MS/MS method employing fragmentation with stepped collision energy for monophosphoryl lipid A containing 3-deoxy-D-manno-octulosonic acid and its derivatives. *Journal of Chromatography A*, *1780*, 467040.